Chapter 1
Image Processing for Localization and Parameterization of the Glandular Ducts of Colon in Inflammatory Bowel Diseases

Stanislaw Osowski
Warsaw University of Technology & Military University of Technology, Poland

Michal Kruk
University of Life Sciences, Poland

Robert Koktysz
Military Institute of Medicine, Poland

Jaroslaw Kurek
University of Life Sciences, Poland

ABSTRACT

This chapter presents the computerized system for automatic analysis of the medical image of the colon biopsy, able to extract the important diagnostic knowledge useful for supporting the medical diagnosis of the inflammatory bowel diseases. Application of the artificial intelligence methods included in the developed automatic system allowed the authors to obtain the unique numerical results, impossible for achieving at the visual inspection of the image by the human expert. The developed system enabled the authors to perform all steps in an automatic way, including the segmentation of the image, leading to the extraction of all glandular ducts, parameterization of the individual ducts and creation of the diagnostic features, as well as characterizing the recognition problem. These features put to the input of SVM classifier enable to associate them with the stage of development of the inflammation. The numerical experiments have shown that the system is able to process successfully the images at different stages of development of the inflammation. Its important advantage is automation of this very difficult work, not possible to be done manually, even by a human expert.

DOI: 10.4018/978-1-60960-551-3.ch001

Copyright © 2011, IGI Global. Copying or distributing in print or electronic forms without written permission of IGI Global is prohibited.

INTRODUCTION

In medicine the inflammatory bowel disease (IBD), for example Crohn's disease and ulcerative colitis, form a group of inflammatory conditions of the large and small intestines (Carpenter & Talley, 200), (Carter et al. 2004). The important problem is to diagnose the beginning of the illness, i.e. the point, when the glandular ducts are attacked by the human defense system. As a result of such attack the shape and other parameters describing the geometry of ducts are changing. The important consequence of this attack is the appearance of the liquid in the stroma of the tissue, extension of the area between the neighboring glandular ducts, as well as beginning of the division process of the glandular ducts (Carpenter & Talley, 2000).

These facts may be discovered in the image of the biopsy of the colon tissue. Analyzing such image we are trying to extract the information of IBD that is contained in it, especially to associate different stages of IBD with the location, shapes, geometry and parameters of the ducts. Especially challenging is to associate the stage of development of IBD with some parameters of ducts. Knowing this association we will be able to build an automatic system supporting the medical expert in his diagnosis.

Figure 1 presents the image of the biopsy of the colon tissue at different stages of the IBD. Figure 1a corresponds to the individuals with full remission of disease (no clinical and endoscopic signs of IBD). The ducts are clearly visible. Most of them are of regular elongated shape, placed parallel to each other. The space between ducts are filled in by the stroma, representing the background of the image. At the beginning of the illness corresponding to initial acute stage (Figure 1b) we can observe the changes in the shape of ducts. Some of them are split into separate parts. Figure 1c presents the moderately advanced active phase of illness. The most characteristic symptom of it is further split of the ducts into many separate small size parts, not connected into compact regions. In the heavy state of IBD (Figure 1d) most of the fragmentary parts of ducts have disappeared and are hardly visible in the image. Their place has been taken by the uniform liquid of the stroma.

It is evident that the advancement of IBD is strictly connected with deformation of the shapes of the glandular ducts in the image. The parameters of these shapes may be treated as a measure of advancement of the illness. However it is impossible to determine these parameters by the visual inspection. We have to employ the computer aided image processing, aimed in discovering and recognizing the essential parts of the image and parameterize them. Hence there is a need for development of a specialized computer program able to preprocess such images in order to localize, extract and parameterize the glandular ducts, and in its final stage to classify the analyzed image into appropriate class corresponding to the development stage of IBD. Up to now there are no such systems used in the hospital practice.

This work is concerned with the automatic extraction and parameterization of the glandular ducts existing in the microscopic image of the biopsy of the colon tissue. The computer program should mimic the human intelligence to find out the characteristic features of the image, use them to extract the appropriate parts of interest (the ducts), and then characterize each duct with the proper set of geometrical parameters. These parameters or the features defined on their basis will be used as the input information to the neural classifier, which is responsible for the recognition of the development stage of IBD. In this way the human intelligence is included in the computer program extracting the fragments of the image that contain the most important part of information regarding the inflammation stage and associating them with the recognition of IBD.

As a result of fully computerized analysis of the image we get the main parameters of the glandular ducts, on the basis of which the automatic neural classifier decides what is the intensity of the inflam-

Figure 1. The images of the biopsy of the colon tissue at different stages of IBD illness: (a) full remission of disease, (b) initial acute stage, (c) moderately advanced stage of illness, (d) heavy advanced state of IBD

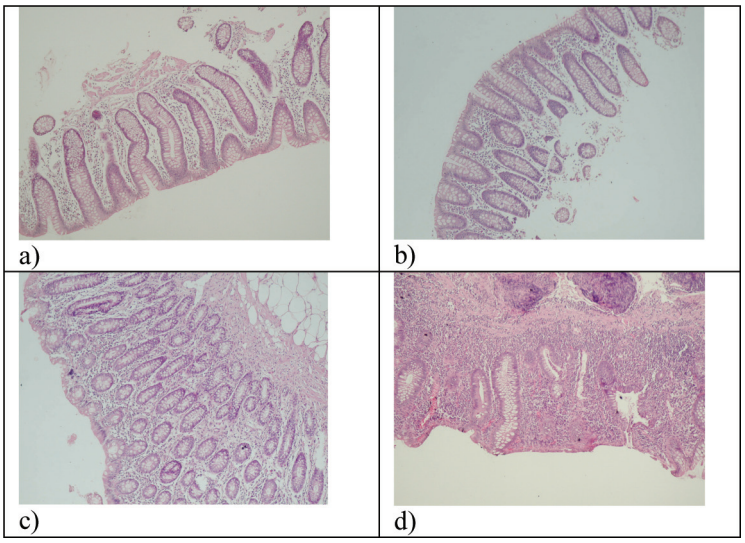

mation. In this way the results of the work may be of great help for medical staff in the process of undertaking the diagnosis of the patients suffering from IBD.

RELATED WORKS

The heart of the proposed solution is the image recognition system, able to perform the successful segmentation and labeling of the individual segments (ducts). The individual segments are transformed into numerical features, which are then associated with the appropriate development stage of the illness through the classification system. Although this particular task defined for the glandular ducts have not been developed yet, there are some related works concerning other biomedical images.

Segmentation of the image is the crucial step in most image recognition systems, especially these devoted to the medical problems. The segmentation of medical images belongs to the most challenging problems due to a large variability in topologies, the complexity of medical structures and poor image modalities such as noise, low contrast, artifacts, etc. Different methods of segmentation have been developed up to day. The most basic are related on edge detection (Duda et al., 2003), (Gonzalez & Woods, 2005), using either approximation of gradient (Sobel, Canny, etc. methods) or the second derivative Laplacian (Kimmel & Bruckstein, 2003).

Thresholding plays also very important role in the segmentation process. The crucial point in thresholding is the proper adjustment of the threshold value. One of the most efficient is the Otsu method (Otsu, 1979), assuming the threshold value separating two classes in a way to minimize the intra-class variance, defined as a weighted sum of variances of the two classes. Another approach is to apply sequential thresholding at different threshold values. This approach is needed at very complex images subject to segmentation. The successful application of this strategy has been developed for segmentation of cells in the image of breast cancer (Markiewicz et. al., 2009).

The segmentation of the image is also possible at application of K-means algorithm. In this approach the task of segmentation is transformed to the classification of different pixels on the basis of their distance to the representative center of the cluster (Duda et al., 2003), (Gonzalez & Woods, 2005). The segmentation may be performed also on some features of the images, being the results of some other preprocessing steps, for example the texture of the image (Markiewicz et. al., 2009).

More efficient are the mathematical morphology approaches, relying the segmentation process on such operations as erosion, dilation, opening and closing (Soille, 2003). On the basis of these operations more complex image processing methods such as watershed algorithm, filling the holes, morphological gradient, reconstruction, etc. have been developed. They have been successfully applied in many solutions regarding biomedical images (Kruk et al., 2007), (Markiewicz et al., 2009).

A popular technique in medical image segmentation is based on a class of deformable models, referred as level set or geodesic active contours (Vasilevskiy & Siddigi, 2002), (Kimmel & Bruckstein, 2003). Recently the variational level set method followed by window-based feature extraction based on PCA and SVM have been proposed (Li et al., 2006). There are also approaches to segmentation combined with denoising, based on the total variation minimization (Chambolle, 2004), (Djemal 2005), (Chan et al., 2006).

After segmenting the image we get the set of objects that are of interest in further image recognition problem. The most important task at this stage is to develop the efficient set of features describing the object in a most discriminative way. In generating features we usually try to follow the human expert by stressing the details, on the basis of which the recognition will be done. In the case of our problem, where the ducts are represented by black and white objects, the most important are the details describing the geometry of these objects (glandular ducts). Among them we may mention the area, perimeter, radius, compactness, concavity, distances between neighboring objects, and the relative coefficients comparing different features (Kruk et al., 2007), (Osowski et.al.2007). These features should characterize the image in a way suppressing the differences within the same class and enhancing them for objects belonging to different classes.

In the case of color medical images many different descriptors may be applied in practice. Among them are the colorimetric descriptors, histograms or texture (Osowski & Markiewicz, 2005), statistical Hu and Zernike moments, 2-D Fourier or wavelet transformation, etc. (Bankman, 2008), (Gonzalez & Woods, 2005). The source of other characterization methods may be found in the books devoted to the pattern recognition (Marraval & Patricio, 2002), (Duda et al., 2003).

The characterization of an image by numerical descriptors results in many features of different quality. Good feature should be stable for samples belonging to the same class (the smallest possible variance) and at the same time it should differ significantly for different classes. The feature assuming similar values for different classes has no discriminative power and may be treated as the noise from the classifier point of view. To get highest possible recognition ratio we have to rely the decision on the most stable and robust features, strictly correlated with the recognized classes. Hence the selection of features is very important on this stage. Many different selection methods have been developed up to day. To the most popular belong principal component analysis, projection pursuit, correlation existing among features, correlation between the features and the classes, analysis of mean and variance of the features belonging to different classes, Fisher LDA. mutual dependence characterization, application of linear SVM or nonlinear feature ranking, etc. Good source of these techniques may be found in (Guyon & Elissseff, 2003), (Lin & Motoda, 2008)

The last step of image recognition is application of an automatic classifier fed by the set of selected features. There are many different solutions of classifier systems used in practice. The simplest Bayesian and KNN classifiers are now pushed out by different types of neural solutions, such as multilayer perceptron (MLP), radial basis function (RBF) networks, neuro-fuzzy networks or Support Vector Machine (SVM). Good review and comparison of these solutions are to be found in excellent textbooks (Haykin, 1999), (Scholkopf & Smola, 2002), (Bishop, 2004). According to the present state of art the most efficient in the classification problems are solutions based on SVM. The structure of SVM is similar to RBF, however its learning algorithm, transforming the problem to the quadratic optimization task is much more efficient and provides better generalization ability (Markiewicz & Osowski, 2005).

The results of all these steps put together in a pipeline fashion create the computer aided diagnosis system, able for the automatic analysis of biomedical images. Although it looks like the universal solution, each case of image analysis has its own peculiarities and needs to treated very carefully. The size of the objects under interest, variability of topologies or poor image modalities force the application of special approach, which guarantee the best possible accuracy of the image recognition.

THE PROPOSED AUTOMATIC SOLUTION FOR DUCT EXTRACTION

The starting point is a microscopic digitized image of the biopsy of the colon tissue at the total magnification equal 100x. The image is saved in the form of a bitmap file. The first step of processing is the extraction of the glandular ducts through the segmentation process connected with the elimination of the other small size elements. The problem is rather complicated, since it should be effective for very different images. Application of linear filters is not efficient due to poor image modalities (low contrast, artifacts and fuzzy character of images). On the other side the level set methods are not directly suitable for clinical image segmentation due to high computational cost, complicated parameter settings and the fact that the convergence of these methods is sensitive to the placement of initial contours (Vasilevskiy & Siddigi, 2002), (Li et al., 2006). One of the possible segmentation solution is also the application of self-organization of pixels on the basis of distances between actual pixels and their prototypes representing either duct or background. However the problem are significant changes of pixels within the duct area.

On the basis of this analysis we have decided to apply the nonlinear image processing, associated with the morphological operations (Gonzales & Woods, 2005), (Soille, 2003), like opening, closing, hole filling, etc. Is known fact, that morphological image processing is successful in segmentation processes (Kruk et al., 2007), Soille, 2003). We have used the morphological operations organized in the pipeline system, applying many times such operations as opening, closing, hole filling and reconstruction. As a result we get the transformed image composed of separate regions containing the separated ducts. Figure 2 presents the general algorithm of extraction of ducts.

The first step is the equalization of the histogram, which emphasizes the details of the image. The equalization is performed by simple rescaling each pixel at the position (x,y) of the original intensity $L(x,y)$ into equalized $L'(x,y)$ according to the equation

$$L'(x,y) = \frac{L(x,y)-1}{L_{\max} - L_{\min}} \left(L(x,y) - L_{\min} \right) \tag{1}$$

Figure 2. The diagram illustrating the algorithm of ducts extraction

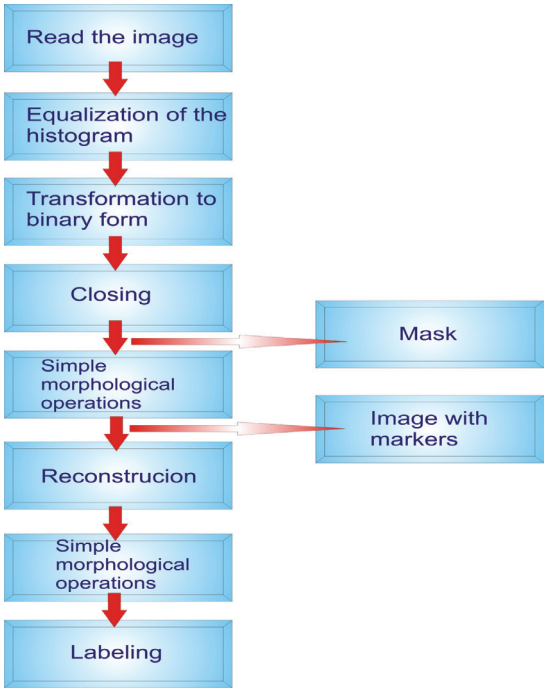

Figure 3. The equalization of the image (a) original image, (b) equalized image

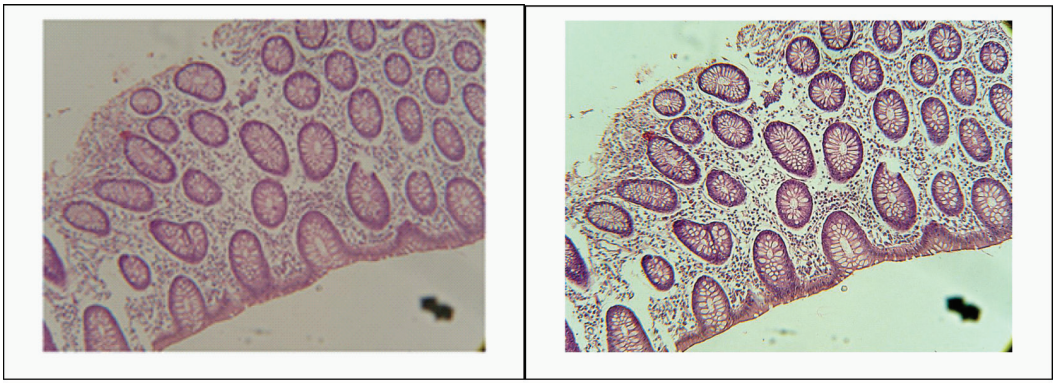

a) b)

where L_{min} and L_{max} represent the minimum and maximal intensity of all pixels. Figure 3 illustrates the original and equalized image of the ducts.

The next operations (the transformation of RBG into binary representation and morphological closing) form the binary mask of the image. In the transformation of the image from RGB to binary we have applied very effective Otsu algorithm (Otsu, 1979), determining the optimal value of bias automatically. To eliminate all tiny elements (the defense cells, the artifact elements of stroma of the tissues, etc.) existing in the image we have applied morphological closing (forming the binary mask) followed by the

Figure 4. The mask (a) and marker form (b) of the transformed image

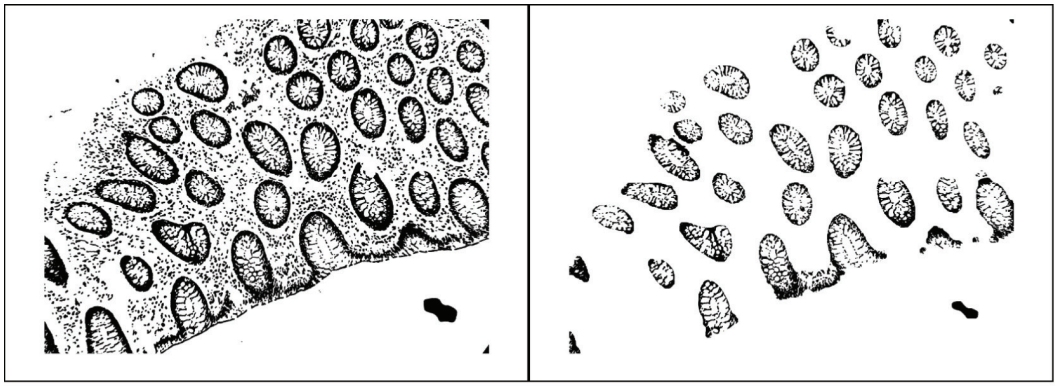

a) b)

hole filling and opening (the marker image). The closing and opening operations were performed by applying the disc structuring element of different sizes: 3 for closing and 7 for opening.

Figure 4 presents the image containing the binary mask (Figure 4a) and marker form (Figure 4b). The markers represent the positions of ducts in the image, on the basis of which we are able to reconstruct full shapes of the ducts.

The mask and markers take part in the next operation called reconstruction (Soille, 2003) of the ducts. This operation recovers the real shape of the ducts while eliminating all small size elements outside them. The next operations consist of series of simple morphological operations performed on the reconstructed image: closing, hole filling and opening. As a result we get the resulting image containing fully filled shapes of discovered ducts, separated from each other. Figure 5 illustrates the reconstructed image (Figure 5a) and the final binary image of duct shapes denoted by different colors (Figure 5b). After labeling each duct we save them as the separate images for further processing.

After segmentation of the image each glandular duct represents the individual image, which must be further processed for creation of its numerical descriptors. In medical diagnosis the most important are the geometrical parameters of these ducts and especially the distances between the nearest glandular ducts. Among the geometrical parameters the most interesting are:

- the real area (A)
- the convex area covered in the polygon circumscribed on a duct (A_c)
- the real perimeter (P)
- the convex perimeter (P_c) defined as the perimeter of the polygon circumscribed on a duct
- the longest (L_l) diameter
- the shortest (L_s) diameters.

The area (A) is the real area covered by the glandular duct (given in pixels). Diameter is the quantity defined in two mutually perpendicular directions. We recognize the long diameter L_l and the short one L_s. The long diameter is the distance (in pixels) between two most distant pixels belonging to the same duct. The short diameter is determined by finding the longest perpendicular line to the long diameter. It

Figure 5. The reconstructed image containing the ducts (a) and the final form of cleaned ducts shapes (b)

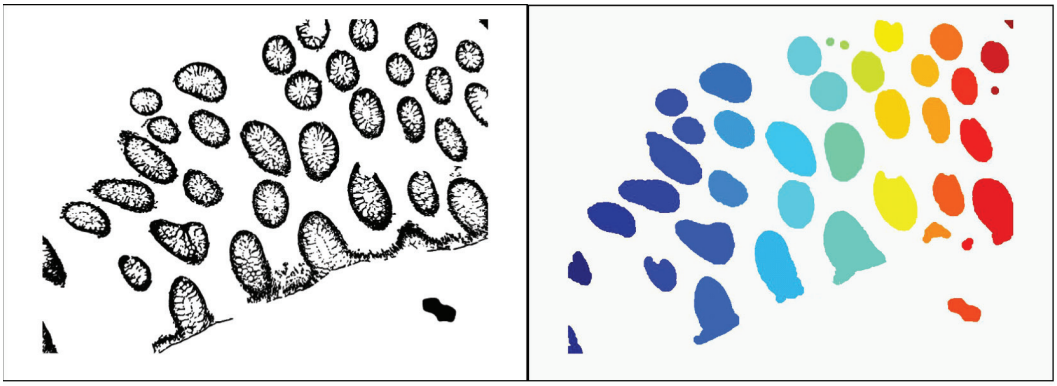

a) b)

is also given in pixels. The real perimeter P is the number of pixels placed on the periphery of the duct (in pixels). The convex perimeter P_c is the perimeter of the polygon circumscribed on a duct. Convex area A_c is the area of the polygon circumscribed on a duct. All of them can be easily computed in an automatic way for each duct, for example using Matlab (Matlab, 2007).

Especially important in the diagnosis are the distances between the neighboring ducts. At the inflammation these distances are higher, because of the liquid appearing in the stroma. To compute automatically these distances between the neighboring glandular ducts we had to develop special algorithm. Once again the human intelligence has been translated into artificial intelligence. The algorithm for distance computation may be presented as following.

- The first step is to find the long diameter of each glandular duct. Its position represents the most important information characterizing the orientation of it in the image.
- After getting the long diameter we draw the series of lines perpendicular to it with the distance of 5 pixels.
- If the perpendicular line intersects the long diameter of the other neighboring glandular duct the distance between the boundary pixels of both ducts are saved.
- Then the mean distance and standard deviation of these distances between the closest neighboring ducts are computed. Standard deviation characterizes the diversity of all distances taken into account in the estimation process. Small value of standard deviation denotes high parallelism of two neighboring ducts.
- The obtained results in the form of the distances between the closest neighboring ducts, the mean distances between them and corresponding standard deviations are saved in the database.

Figure 6b illustrates the applied method of the computation of distances between the neighboring ducts corresponding to the colon tissue image of Figure 6a. The components taken into account at computation of the mean distances between the glandular ducts are visible as the lines between the long diameters. For the purpose of diagnosis only the smallest value of the mean distance between the succeeding ducts and their closest neighbors should be taken into account and saved on a disc.

Figure 6. The illustration of the procedure of computation of distances between the neighbouring glandular ducts: (a) the image of a colon tissue, (b) the extracted duct areas found by the algorithm (labeled by the numbers from 1 to 15) and the lines used in determination of distances between ducts.

a)

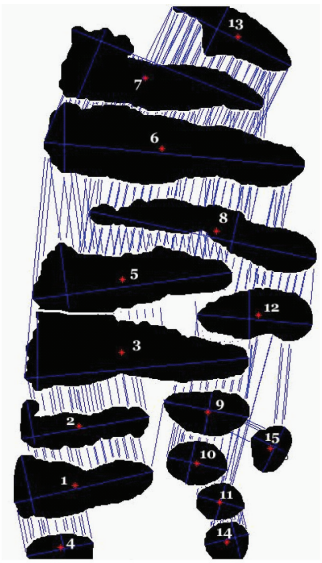

b)

Note that the neighbors of the glandular ducts may vary. For example the closest neighbor for duct No 1 is the duct No 2 and vice versa. However it is not the general rule. For example the closest neighbor of duct No 8 is duct No 12, but for duct No 12 the closest neighbor is duct No 5. Note that neighbors are selected on the basis of the average distances for all lines connecting two ducts. This is the reason, why the ducts No 3 and 5 are not the closest neighbors, although on a short section they are very close to each other.

Table 1 presents the numerical values of the distances and standard deviations between the closest neighboring ducts corresponding to Figure 6. For each glandular duct the mean value of this distance and standard deviation are given. We can see that highly parallel ducts, for example 1 and 2 have very small values of std/mean ratio.

In general the mean values of distances between the neighboring ducts averaged over all pairs of ducts provide the important information of the general inflammation state of the intestines. On the other side the standard deviation characterizes the diversity of all distances that have been taken into account at the estimation process. Small value of standard deviation denotes high parallelism of two neighboring ducts.

Actually all stages of analysis of the image, leading to the extraction and parameterization of glandular ducts are done automatically by the computer and the numerical results are saved in Excel file. The time of full image analysis is very short. For the average image it takes only few seconds on a PC. The developed computerized system of automatic image analysis written in Matlab (Matlab, 2007) is able to do the following steps (Kruk et al., 2007):

Table1.The distances between the glandular ducts

Glandular duct	Neighbouring duct	Mean distance	Std of distances
1	2	121,71	24,76
2	1	121,71	24,76
3	12	83,88	14,28
4	1	160,79	31,28
5	12	71,57	24,37
6	7	62,88	22,11
7	6	62,88	22,11
8	7	97,48	19,62
9	5	162,28	34,89
10	11	123.17	29,13
11	10	123.17	29,14
12	5	74,57	22,54
13	10	84,04	18,79
14	13	137,04	27,82
15	11	120,09	25,42

- reading and saving the whole image of biopsy on the disc
- segmentation and extraction of all glandular ducts appearing in the image
- measuring the distances between the neighboring ducts
- determination of the other geometrical parameters of the ducts mentioned in the text
- saving the results of parameterization on the disc in the form of Excel file
- putting the binary images of the ducts in the archive graphical files for future use.

The developed system is able to do all these steps automatically (without intervention of the human operator) for the images corresponding to the first step of illness development. In the case of more advanced stages the automatic interpretation of the image may be difficult and sometimes there is a need for intervention of the human operator (to cut some connection of the ducts with the stroma of the tissue, not properly segmented by the automatic system). This operation is also supported by the handy graphical user interface developed by us.

THE AUTOMATIC SYSTEM FOR CLASSIFICATION OF THE DEVELOPMENT STAGE OF IBD

After extraction and parameterization of the ducts it is possible to build an automatic classification system able to recognize among three mentioned stages of illness. The idea is to develop some set of numerical descriptors based on the estimated geometrical parameters of the ducts that well characterizes different stages of IBD development. Two tasks should be solved at this stage.

- Definition of the most representative descriptors (features) that are able to separate different classes of illness.
- Application of automatic classification system of highest possible efficiency, able to recognize patterns characteristic for different stages of illness.

To get good results of recognition we have to develop the features well representing the patterns characteristic for each stage of illness. On the basis of them the classifier will generate its most accurate decision concerning the final recognition. Good feature should be very stable for samples belonging to the same class (the smallest possible variance) and at the same time it should differ significantly for different classes. To distinguish between these classes, the positions of means of feature values for the data belonging to different classes should be separated as much as possible. The feature of the standard deviation value much higher than the distance between two neighboring class centers is useless for these two particular classes recognition, since it does not distinguish between them. It has no discriminative power and may be treated as the noise from the classification point of view. Thus the main problem in classification is to find out the efficient methods of selection of features according to their importance for the problem solution (Duda et al., 2003), (Guyon & Elisseff, 2003). In our solution we have applied Fisher measure, since it directly incorporates our demand for the separation of features describing different classes. For two classes A and B Fisher discrimination coefficient of the feature f is defined as follows

$$S_{AB}(f) = \frac{\left|c_A(f) - c_B(f)\right|}{\sigma_A(f) + \sigma_B(f)} \tag{2}$$

In this definition c_A and c_B are the mean values of the feature f in the class A and B, respectively. The variables σ_A and σ_B represent the standard deviations determined for both classes. The large value of $S_{AB}(f)$ indicates good potential separation ability of the feature f for these two classes. On the other side small value of it means that this particular feature is not good for the recognition between classes A and B. In the case of many classes recognized by application of the same set of feature, the usefulness of each of them may be measured by the sum of S_{AB} over all pairs of classes (A,B).

After determination of the most important features the next problem is to chose the most effective automatic classifier, which would be able to recognize the class on the basis of these features. Among many existing classifiers, like Bayes, distance classifiers, classical neural networks and support vector machines (SVM). The SVM is commonly regarded as the most effective solution (Haykin, 1999), (Scholkopf & Smola, 2002). This is the reason why we have chosen SVM as the classifying tool.

The learning problem of SVM is formulated as the task of separating learning vectors $\mathbf{x}_i$ (i=1, 2,..., p) into two classes of the destination values either $d_i=1$ (one class) or $d_i=-1$ (the opposite class) with the maximal separation margin (Scholkopf & Smola, 2002), (Vapnik, 1998). Applying the Lagrangian approach this primary task is transformed to the so called dual problem of maximization of the quadratic function $Q(\pm)$ with respect to the Lagrange multipliers α_i, defined in the way (Scholkopf & Smola, 2002)

$$\max \quad Q(\alpha) = \sum_{i=1}^{p} \alpha_i - \frac{1}{2}\sum_{i=1}^{p}\sum_{j=1}^{p} \alpha_i \alpha_j d_i d_j K\left(\mathbf{x}_i, \mathbf{x}_j\right) \tag{3}$$

with the constraints

$$\sum_{i=1}^{p} \alpha_i d_i = 0 \qquad 0 \le \alpha_i \le C \tag{4}$$

In this formulation C is the regularization constant, defined by the user, p - the number of learning data pairs ($\mathbf{x}_i$, d_i) and $K(\mathbf{x},\mathbf{x}_i)$ is the kernel function fulfilling Mercer conditions (Vapnik, 1998). As it is seen the learning task is transformed to the solution of the quadratic optimization problem, which has many, very efficient implementations. In practice we have applied the modified sequential programming algorithm (Hsu & Lin, 2002), (Scholkopf & Smola, 2002).

The important point in designing SVM classifier is the choice of kernel function. The simplest linear kernel was inefficient due to the lack of linear separability of the data. The polynomial kernel checked in the introductory experiments was found also useless, since high degree of polynomial was needed and the system had become badly conditioned. The most often used is the Gaussian kernel defined in the form $K(\mathbf{x}, \mathbf{x}_i) = \exp\left(-\gamma \left\|\mathbf{x} - \mathbf{x}_i\right\|^2\right)$, where γ is the hyperparameter chosen by the user. In our experiments we have applied this kernel.

The regularization coefficient C determines the balance between the complexity of the network, characterized by the weight vector $\mathbf{w}$ and the error of classification of learning data. Low value of C means smaller significance of the learning errors in the adaptation stage. For the normalized input signals the value of C is usually much bigger than one. Its optimal value is usually determined after a series of experiments via the standard use of the validation test set. For normalized data the typical value of C is in the range (100, 1000). The process of optimizing the values of C and γ is done together. Many different values of C and γ combined together in the learning process have been used in the learning process. Their optimal values are those for which the classification error on the validation data set (small part of learning set) is the smallest one.

The decision function of the classifier associating the input vector $\mathbf{x}$ with a class is relied on the output signal $y(\mathbf{x})$ of the SVM, where this signal is determined by (Scholkopf & Smola, 2002)

$$y(\mathbf{x}) = \sum_{i=1}^{N_{sv}} \alpha_i d_i K(\mathbf{x}_i, \mathbf{x}) + b \tag{5}$$

N_{sv} is the number of support vectors (the vectors $\mathbf{x}_i$ for which the Lagrange multipliers are different from zero). The positive value of the output signal $y(\mathbf{x})$ is associated with the first class and the negative with the opposite one. To deal with a problem of many classes we have used one against one approach (Hsu & Lin, 2002). In this approach the SVM networks are trained to recognize between all combinations of two classes of data. For M classes we have to train $M(M\text{-}1)/2$ individual SVM networks. In the retrieval mode the vector $\mathbf{x}$ belongs to the class of the highest number of winnings in all combinations of classes.

RESULTS OF EXPERIMENTS

Using the developed system we have checked 197 images of the intestine biopsies prepared for the patients of different stages of development of IBD. Among them 26 belonged to individuals in remission phase in which the patients underwent biopsy due to other diseases, 61 – initial acute stage, and the highest number (110) to the advanced active stage of IBD development. These were the number of patients available to date in the data base of the hospital. Especially small is the group of individuals with full remission of disease, since this group of people is generally not subject to such investigation. As a result of all image preprocessing we have extracted 2944 glandular ducts. Only in the most difficult cases corresponding mainly to the heavy advancement of illness the manual intervention of human operator was needed in the extraction process. However such images represented not more than 5% of all images in the data base. All extracted ducts have been labeled and saved on the disc.

The applied image processing has resulted in two kinds of outcome. The first one is in the graphical form of extracted ducts and the second - in the numerical forms of geometrical parameter values associated with each extracted ducts. The numerical data have been saved in Excel file. Further analysis of these parameters using SVM classifier has allowed to associate them with the stage of development of IBD.

Graphical Form of Output

The graphical results of image processing correspond to all investigated stages of IBD. Figure 7 presents three examples of images processed fully automatically by our processing system (without any intervention of the human operator). They cover all stages of IBD development.

As it is seen all glandular ducts have been extracted practically in a perfect way. All of them have been labeled automatically by our system and saved on a disc in the form of a graphical file.

Figure 8 presents the set of images, where some intervention of the human operator in the processing of the image was needed. The main difficulties in automatic analysis of these images were either the changes of illumination of some parts of the image (the upper image) or advanced stage of inflammation causing the stroma and defense cells create the structure resembling the ducts (the middle and lower images of Figure 8).

The quality of an automatic extraction of ducts was satisfactory from the medical point of view. Their quantity found in the image as well as the shape of each duct were in good agreement with the human expert assessment. This means that the graphical results may stand good basis for further medical investigations directed to the parameterization of the ducts.

Parameterization of Ducts

The medical researchers are looking for the numerical measures that are strictly associated with the advancement of IBD. To these measures belong first of all the geometrical parameters of the ducts. They form the potential diagnostic features. To get reliable recognition system we should search for the reasonably large set of them, characterizing the problem from different points of view. Sufficiently high number of features provides perspective of good characterization of the process of image recognition. However among automatically generated features there might be some not well discriminating different classes, and hence useless from the recognition point of view. Note that the features assuming the same

Figure 7. The examples of images processed automatically by our system without intervention of the human operator: left column – the original image, right column – the extracted glandular ducts generated by the system. The images in the middle row represent the initial acute stage of IBD and the other images – the advanced active phase.

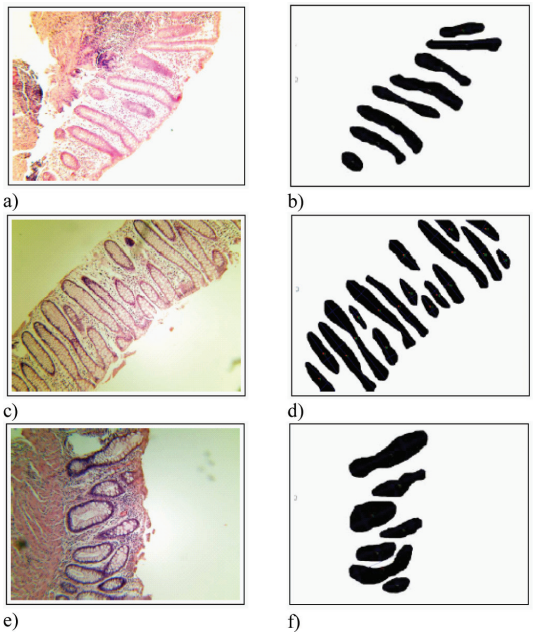

Figure 8. The examples of images processed semi-automatically with some help of human operator (all of them belonged to advanced active phase of IBD): left column – the original images, right column – the extracted glandular ducts.

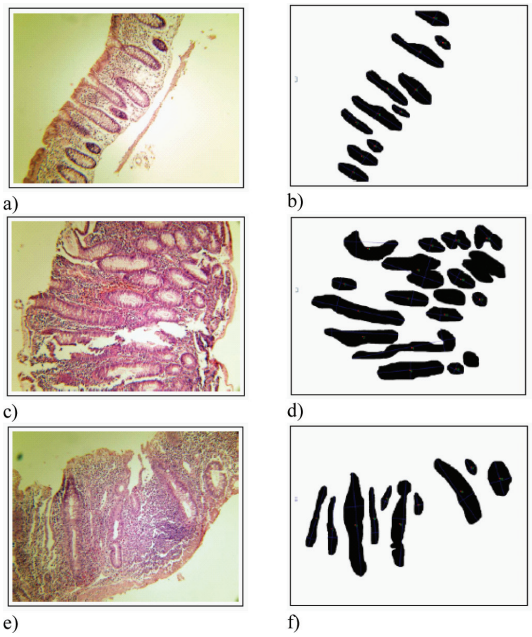

values for different classes have no discriminative properties. The same could be said about the features of the values interlacing for different classes or are largely dispersed.

The digital image processing tools developed in the form of the computer program allow to find the candidates for diagnostic features in an automatic way. The easiest way of assessing the class discriminative abilities of the individual features is to study their mean and standard deviation for the particular class. Table 2 presents the results of determination of the distances D between the neighboring ducts (one of the most important factors checked by the medical expert) and the basic geometrical parameters (the real area A, compact area A_c, the perimeter P, the convex perimeter P_c, long diameter L_l, and short diameter L_s) for three chosen patients belonging to three representative groups: class 1 - individuals with full remission of disease, class 2 – the initial acute stage and class 3 - the advanced active phase. We present the mean values and standard deviations (std) for all ducts existing in the image corresponding to each patient (all expressed in pixels)

The analysis of these results can deliver quite important information for supporting the medical diagnosis. First of all we can see that the mean distances between the neighboring ducts are generally larger at more advanced stages of illness. Besides this the values of the standard deviation are less stable at the advanced stage of IBD. These particular results of the mean distances confirm good correlation of the averaged mean distances between the neighboring ducts and the stage of development of the inflammation for the chosen individuals. It means that the information regarding the mean distances between

Table 2. The mean values and standard deviations (std) of the geometrical parameters of all ducts in the image calculated for three kinds of patients: class 1 - individuals with full remission of disease, class 2 – the initial acute stage and class 3 - the advanced active phase

Patients			D	A	A_c	P	P_c	L_l	L_s
Class 1	P332	mean	69.3	41831	43352	732	626	348	141
		std	15.00	29233	31024	321	300	172	30
	P331	mean	73.4	43652	45442	749	600	337	162
		std	17.02	18175	20695	208	178	102	33
	P327	mean	76.2	44930	52219	870	681	393	142
		std	20.08	29062	38263	351	300	187	27
Class 2	P326	mean	92.4	37451	39502	724	590	318	149
		std	19.96	16423	18490	229	218	108	46
	P330	mean	87.1	63058	73250	1122	997	521	152
		std	23.03	32540	39927	420	406	216	44
	P325	mean	80.57	21267	22115	507	377	208	133
		std	12.65	10832	11582	154	137	86	18
Class 3	P328	mean	133.1	107421	130113	1413	1233	678	214
		std	45.01	62965	91720	697	671	349	31
	P323	mean	112.5	78198	90157	1360	1233	673	137
		std	25.80	31969	38965	415	414	216	32
	P329	mean	107.4	65434	69290	981	839	461	172
		std	24.01	46081	50829	473	422	266	44

the neighboring ducts may be a good indication of the stage of inflammation of the intestines and provide the important factor at the assessment of the stage of illness.

The other geometrical parameters presented in Table II for the same representatives of these three groups of patients are not so easily conclusive. There is a large variety of these values, which change greatly for patients belonging to the same group and also between groups. Note also large values of standard deviations of these parameters (usually half or even more of the mean). These large values are the evidence of high variability of parameters of the individual ducts existing in the analyzed images.

To confirm these observations we have performed the same calculations for all patients belonging to these three groups of interest (class 1 - 26 individuals, class 2 – 61 individuals, class 3 - 110 individuals). Table 3 presents the statistics of these investigations in the form of mean values and standard deviations of these parameters.

Looking at these statistical results we can see quite large variability of most of the statistical parameters, undermining their usefulness in the diagnosis process. The most stable are only the results concerning the average distances between the neighboring ducts (parameter *D*), making this parameter very important in the diagnosis. Moreover most of the average parameters (except *D*) characterizing each group of patients are very close to each other. It means that these parameters are not appropriate for recognition of the stage of advancement of illness.

Analyzing the detailed numerical results of parameterization for the whole set of images of patients belonging to these three classes we have tried to find another, more stable characterization of patients, relying on the ratio of some of them. Close analysis of the details of results concerning the data base of parameters has enabled to reveal some other more stable descriptors in the form of appropriate ratios, that are defined on the basis of the crude values obtained from the parameterization. We have introduced the following descriptors defined in the form of the ratio of the appropriate geometrical parameters:

circularity factor F_c

$$F_c = \frac{4\pi A}{P} \tag{6}$$

factor of convex circularity F_{cc}

$$F_{cc} = \frac{4\pi A_C}{P_C} \tag{7}$$

homogeneity factor F_h

$$F_h = \frac{P^2}{A} \tag{8}$$

factor of convex homogeneity F_{ch}

Table 3. The mean values and standard deviations (std) of the geometrical parameters of all ducts in the image calculated for the whole population of investigated patients forming the group of 3 classes

Group of patients		A	A_c	P	P_c	L_l	L_s	D
Class 1	mean	85501.37	87338.30	1259.22	1198.33	448.90	176.18	87.08
	std	34375.66	37579.30	285.88	263.98	143.21	44.28	28.06
Class 2	mean	91959.45	108684.27	1450.17	1134.70	522.72	189.01	103.70
	std	46137.06	53353.85	341.66	286.84	154.67	62.19	38.39
Class 3	mean	101359.44	149697.75	1608.01	1166.66	505.72	185.03	160.42
	std	27175.90	37378.06	351.13	200.64	176.05	15.06	30.56

$$F_{ch} = \frac{P_c^2}{A_c} \tag{9}$$

corrugation factor F_{cr}

$$F_{cr} = \frac{P_c}{P} \tag{10}$$

factor of ruggedness F_r

$$F_r = \frac{A}{A_c} \tag{11}$$

number N of ducts in the image of the normalized size

They represent the potential features used in the recognition of the stage of advancement of illness. In Table 4 we present the statistical results (means and standard deviations) concerning these features calculated for the whole data base of the analyzed images.

Comparing the values of the mean and standard deviation of these descriptors we can observe the significant improvement. The mutual distances between their means corresponding to three stages of development of IBD are now much larger, while the standard deviations of the feature within the same group is smaller.

To assess the discrimination ability of the developed descriptors in a most objective way we have used the Fisher measure described by (2).This measure is defined for each feature f and for each pair of classes under recognition: $S_{12}(f)$, $S_{13}(f)$ and $S_{23}(f)$. Table 5 presents the values of Fisher measure for each of the candidate features: D, F_c, F_{cc}, F_h, F_{ch}, F_{cr}, F_r and N, at recognition of two class problems. The first row of results corresponds to recognition of the first two classes, second row – the classes 1 and 3 and the third row – classes 2 and 3. Since the same features will be taken into account in assessment of each image we have to rely in our choice on the sum of Fisher measures concerning all compared pairs of

Table 4. The mean values and standard deviations (std) of the relative factors characterizing of all ducts in the image calculated for the whole population of investigated patients forming the group of individuals with full remission of disease (class 1), initial acute stage (class 2) and the advanced active phase of IBD development (class 3)

Group of patients		*D*	F_c	F_{cc}	F_h	F_{ch}	F_{cr}	F_r	*N*
Class 1	mean	87.08	853.25	915.87	18.54	16.44	0.95	0.97	15
	std	28.06	112.21	102.87	3.78	3.32	0.11	0.14	5
Class 2	mean	103.70	796.86	1203.63	22.86	11.84	0.78	0.84	18
	std	38.39	116.76	132.54	4.23	2.79	0.09	0.11	7
Class 3	mean	160.42	792.10	1612.43	25.51	9.09	0.72	0.67	6
	std	30.56	176.65	234.76	4.78	2.21	0.09	0.07	3

Table 5. The values of Fisher measure of the discrimination ability for the set of features at recognition of pairs of classes.

	D	F_c	F_{cc}	F_h	F_{ch}	F_{cr}	F_r	*N*
S_{12}(f)	0.2501	0.2463	1.2224	0.5393	0.7529	0.8500	0.5200	0.2500
S_{13}(f)	1.2511	0.2117	2.0631	0.8143	1.3291	1.1500	1.4286	1.1250
S_{23}(f)	0.8226	0.0162	1.1130	0.2941	0.5500	0.3333	0.9444	1.2000
Sum	2.3238	0.4742	4.3985	1.6477	2.6320	2.3333	2.8930	2.5750

classes. Hence in the fourth row we show the total discrimination power of each descriptor expressed as the sum of elements in the appropriate column.

It is seen now that the best descriptor (corresponding to the largest value of the summed Fisher measures) is the factor of convex circularity F_{cc}. Its total value 4.3985 is almost twice higher than the next one. Moreover it is almost equally good for recognition between each pair of classes. Evidently the worst one is the circularity factor F_c, which seems to be useless at recognition of any pair of classes (very small value of Fisher measure for all pairs of classes). On the basis of this analysis we have decided to exclude this descriptor from the applied feature set used in automatic recognition of the state of inflammation. So the input vector to the classifier is composed of 7 remaining features.

Automatic Recognition of the Intensity of Inflammation

In the next experiments we have checked how the selected features are efficient in automatic recognition of the stage of IBD development. Many different solutions of classification system may be applied. Nowadays the most effective are the neural like classifiers, such as MLP, RBF, neuro-fuzzy or SVM. According to our experience and very detailed comparisons made by researchers (Meyer et al., 2003) the most effective classifier is SVM. The PCA analysis of distribution of features has shown, that the data are not linearly separable, thus the nonlinear kernel SVM is needed. The SVM classifier of Gaussian kernel function was selected. This kind of solution is very similar to RBF with respect to the structure,

Table 6. The average confusion matrix of the IBD stage recognition (in relative terms) corresponding to 20 trials

Class	1	2	3
1	94.1%	2.63%	3.27%
2	3.35%	92.26%	4.19%
3	0	2.63%	97.37%

but of absolutely different principle of learning algorithm. The detailed comparison of it with RBF (Markiewicz & Osowski, 2005) has shown the superiority of SVM.

The important step in learning is the choice of hyperparameters C (the regularization constant) and γ (the parameter of Gaussian function). These hyperparameters have been adjusted by trying the limited set of predefined values and choosing the values corresponding to best results on the validation set (20% of the learning data). The optimal values of them were found as follows C=200 and γ=0.01. To get the most objective results of testing we have applied the cross validation approach. From the available data 2/3 of the set have been used in learning of SVM and the remaining 1/3 were left for testing purposes. The learning stage of SVM is extremely quick. The average time of learning the SVM classifier system was about 3 seconds. The experiments of learning and testing have been repeated 20 times at random choice of both subsets. As the vector **x,** applied to the input of the SVM classifier we have assumed the seven element vector containing the most important features $\mathbf{x}=[F_{cc}, F_r, F_{ch}, N, F_{cr}, D, F_h]$, chosen according to summed Fisher measures gathered in Table 5.

Table 6 presents the average results of recognition of each class on the testing data not taking part in learning. The results are in the form of confusion matrix representing the average values of recognition ratio obtained at 20 runs of experiments in cross correlation mode. The diagonal entries of this matrix represent right recognition of the class and the off diagonal – the misclassification ratios (all expressed in percentage). The row presents how the particular class has been classified. The column indicates which class has been classified as the type mentioned in this column. The results of Table 6 point directly what was the accuracy of recognition of each class and what is the average misclassification ratio.

The average accuracy of recognition of the first class among all other cases was equal 94.1%, for the second class - 92.26% and of the third one - 97.37%. If we calculate the relative error as the ratio of the number of all misclassifications to the total number of cases we get the mean value in all experiment equal 4.59% at standard deviation of 2.68%. For comparison we made similar experiments with other neural classifiers. At application of MLP of the optimal structure 7-8-3 the total misclassification rate on the same data base was equal 6.27%. Application of RBF resulted in the total relative error equal 5.92%.

The most striking observation is the relative high value of misclassification of the samples belonging to the first class (full remission of disease). This is due to the small number of learning data of this class used in experiments (most of the investigated patients were ill). The population of the representatives of three investigated classes was highly unbalanced (only 26 samples representing the first class in comparison to 110 of the third one). However notice, that none of the patients in an advanced stage (class 3) was misclassified with class one (full remission of disease).

FUTURE RESEARCH DIRECTIONS

The research presented in the chapter has shown the way of automation of the process of recognition of different stages of IBD. However a lot of additional research should be done before applying it in the medical practice.

- Much larger data base of cases should be collected in the hospital and used in testing to find the most objective assessment of the real efficiency of the proposed system. Extending the data base we should take care of balancing the cases belonging to different classes.
- Additional attention should be paid to find another diagnostic features of good class separation ability. At large number of such features the selection of the best features should be done as an additional step. As a selection tools we may apply not only Fisher measure but also more advanced algorithms, for example application of SVM.
- The next direction is to apply many classifiers arranged in an ensemble. It is well known that efficiency of the ensemble is higher than individual classifier. These classifiers may be build on the basis of Gaussian kernel SVMs by applying as input information to each of them the limited number of diagnostic features selected randomly from the whole set of best features.
- The additional research problem is the optimal integration of the ensemble. The classical majority voting, weighted majority voting, different forms of naïve Bayes approaches, principal component approach, as well as Kullback-Leibler divergence methods are the examples of solution that might be applied.

CONCLUSION

The work has presented the computerized system directed to extracting the important diagnostic knowledge contained in the medical image of the colon biopsy. In creating it we have mimicked the way the human expert assesses the image. Application of the artificial intelligence included in the developed automatic system allows to obtain the unique numerical results, not possible for achieving at the visual inspection of the image by the human expert.

The system is able to extract the ducts at different stages of development of the inflammation. Its important advantage is automation of this very difficult and responsible work, not possible to be done manually by the human expert. The developed system has been applied to the analysis of 197 medical images corresponding to different stages of IBD. In most investigated cases the system was able to extract the ducts automatically and there was no need for human operator to intervene. Only in the case of heavy advancement of illness the human intervention in the image processing was sometimes needed to obtain the accurate results of extraction.

The most important results are concerning the numerical characterization of the glandular ducts, enabling to apply them as the input information for automatic neural type classifier, able to recognize the stage of advancement of the illness. The numerical experiments performed at the application of SVM as a classifier have shown very encouraging results, confirming the hope to develop an efficient tool for supporting the medical diagnosis of IBD.

The developed system allows to analyze the colon images in a very short time, delivering the readable results in a very convenient form. Thanks to this it may present very efficient tool for medical

scientists involved in investigation of hundreds of cases of IBD, enabling to accelerate the research in this important medical area.

REFERENCES

Bishop, C. (2006). *Pattern recognition and machine learning*. Singapore: Springer.

Carpenter, H., & Talley, N. (2000). The importance of clinicopathological correlation in the diagnosis of inflammatory conditions of the colon. *The American Journal of Gastroenterology*, *95*, 234–245. doi:10.1111/j.1572-0241.2000.01924.x

Carter, M., Lobo, A., & Travis, S. (2004). Guidelines for the management of IBD for adults. *British Society of Gastroenterology*, *53*, 1–16.

Chambolle, A. (2004). An algorithm for total variation minimization and applications. *Journal of Mathematical Imaging and Vision*, *20*, 89–97. doi:10.1023/B:JMIV.0000011321.19549.88

Chan, T., Esedoglu, S., & Nikolova, M. (2006). Algorithms for finding global minimizers of image segmentation and denoising models. *SIAM Journal on Applied Mathematics*, *66*, 1632–1648. doi:10.1137/040615286

Djemal, K. (2005). *Speckle reduction in ultrasound images by minimization of total variation.* International Conference on Image Processing, Sousse, Tunisia.

Duda, R. O., Hart, P. E., & Stork, P. (2003). *Pattern classification and scene analysis*. New York, NY: Wiley.

Gonzalez, R. C., & Woods, R. E. (2005). *Digital image processing*. Reading, MA: Addison-Wesley.

Guyon, I., & Elisseeff, A. (2003). An introduction to variable and feature selection. *Journal of Machine Learning Research*, *3*, 1158–1182. doi:10.1162/153244303322753616

Haykin, S. (1999). *Neural networks-a comprehensive foundation*. New York, NY: Macmillan.

Hsu, C. W., & Lin, C. J. (2002). A comparison method for multi class support vector machines. *IEEE Transactions on Neural Networks*, *13*, 415–425. doi:10.1109/72.991427

Bankman, I. N. (Ed.). (2008). *Handbook of medical image processing and analysis*. Boston, MA: Academic Press.

Kimmel, R., & Bruckstein, A. M. (2003). Regularized Laplacian zero crossings as optimal edge integrators. *International Journal of Computer Vision*, *53*, 225–243. doi:10.1023/A:1023030907417

Kruk, M., Osowski, S., & Koktysz, R. (2007). Segmentation and characterization of glandular ducts in microscopic colon image. *Przeglad Elektrotechniczny*, *84*, 227–230.

Li, S., Fevens, T., & Krzyzak, A. (2006). Automatic clinical image segmentation using pathological modeling, PCA and SVM. *Engineering Applications of Artificial Intelligence*, *19*, 403–410. doi:10.1016/j.engappai.2006.01.011

Liu, H., & Motoda, H. (2008). *Computational methods of feature selection*. London, UK: Chapman.

Markiewicz, T., Wisniewski, P., Osowski, S., Patera, J., Kozlowski, W., & Koktysz, R. (2009). Comparative analysis of the methods for accurate recognition of cells in the nuclei staining of the Ki-67 in neuroblastoma and ER/PR status staining in breast cancer. *Analytical and Quantitative Cytology and Histology Journal*, *31*, 49–63.

Markiewicz, T., & Osowski, S. (2005). *OLS versus SVM approach to learning of RBF networks*. International Joint Neural Network Conference, Montreal, (pp. 1051-1056).

Marraval, D., & Patricio, M. (2002). Image segmentation and pattern recognition. In Chen, D., & Cheng, X. (Eds.), *Pattern recognition and string matching*. Amsterdam, The Netherlands: Kluwer.

Meyer, D., Leisch, F., & Hornik, K. (2003). The support vector machine under test. *Neurocomputing*, *55*, 169–186. doi:10.1016/S0925-2312(03)00431-4

(2007). *Image Processing toolbox - Matlab user manual*. Natick, MA: MathWorks.

Osowski, S., & Markiewicz, T. (2007). Support vector machine for recognition of white blood cells in leukemia. In Camps-Valls, G., Rojo-Alvarez, J. L., & Martinez-Ramon, M. (Eds.), *Kernel methods in bioengineering, signal and image processing* (pp. 93–123). Hershey, PA: Idea Group Publishing. doi:10.4018/9781599040424.ch004

Otsu, N. (1979). A threshold selection method from grey-level histograms. *IEEE Transactions on Systems, Man, and Cybernetics*, *9*, 62–66. doi:10.1109/TSMC.1979.4310076

Schölkopf, B., & Smola, A. (2002). *Learning with kernels*. Cambridge, MA: MIT Press.

Soille, P. (2003). *Morphological image analysis, principles and applications*. Berlin, Germany: Springer.

Vasilevskiy, A., & Siddigi, K. (2002). Flux maximizing geometric flow. *IEEE Transactions of PAMI*, *24*, 1565–1578.

Vapnik, V. (1998). *Statistical learning theory*. New York, NY: Wiley.

ADDITIONAL READING

Bartlett, P., & Traskin, M. (2008). AdaBoost is Consistent. *Journal of Machine Learning Research, Vol.*, *9*, 2347–2368.

Corani, G., & Zaffalon, M. (2008). Learning Reliable Classifiers From Small or Incomplete Data Sets: The Naive Credal Classifier 2. *Journal of Machine Learning Research*, *9*, 581–621.

Demirkaya, O., & Asyali, M. H. (2009). *Image processing with Matlab application in medicine and biology*. London: CRC.

El-Naqa, I., Yang, Y., Wernick, M. N., Galatsanos, N. P., & Nishikawa, R. M. (2002). A support vector machine approach for detection of micro calcifications. *IEEE Transactions on Medical Imaging*, *21*, 1552–1563. doi:10.1109/TMI.2002.806569

Gonzalez, R. C. Woods R. E, & Eddins S. L. (2009*). Digital Image Processing Using MATLAB*. Upper Saddle River, Prentice Hall.

Guyon, I., Weston, J., Barnhill, S., & Vapnik, V. (2002). Gene selection for cancer classification using Support Vector Machines. *Machine Learning*, *46*, 389–422. doi:10.1023/A:1012487302797

Heijmans, H. J., & Roerdink, J. B. (1998). *Mathematical Morphology and its Applications to Image and Signal Processing* (eds). Dordrecht, Kluwer Academic Publishers.

Heijmans, H. J. (1999). Connected Morphological Operators for Binary Images. *Computer Vision and Image Understanding*, *73*, 99–120. doi:10.1006/cviu.1998.0703

Kotsiantis, S. B., & Pintelas, P. E. (2004). Combining bagging and boosting. *Intern. J. of Computational Intelligence*, *1*, 324–333.

Kruk, M., Osowski, S., & Koktysz, R. (2009). Recognition and Classification of Colon Cells Applying the Ensemble of Classifiers. *Computers in Biology and Medicine*, *39*, 156–165. doi:10.1016/j.compbiomed.2008.12.001

Krupka, E., Navot, A., & Tishbt, N. (2008). Learning to select features using their properties. *Journal of Machine Learning Research*, *9*, 2349–2376.

Kuncheva, L. (2004). *Combining pattern classifiers: methods and algorithms*. New Jersey: Wiley. doi:10.1002/0471660264

Liu, H., & Motoda, H. (2008). *Computational methods of feature selection*. London: Chapman & Hall/CRC.

Liu, Y. (2004). A Comparative Study on Feature Selection Methods for Drug Discovery. *Journal of Chemical Information and Computer Sciences*, *44*, 1823–1828. doi:10.1021/ci049875d

Mitra, S., & Acharya, T. (2003). *Data mining*. New York: Wiley.

Muthu, R. K., Pal, M., Bomminayuni, S. K., Chakraborty, C., & Paul, R. R. (2009). Automated classification of cells in sub-epithelial connective tissue of oral sub-mucous fibrosis—An SVM based approach. *Computers in Biology and Medicine*, *39*, 1096–1104. doi:10.1016/j.compbiomed.2009.09.004

Najarian, K., & Splinter, R. (2005). *Biomedical Signal and Image Processing*. London: Taylor & Francis.

Nixon, M., & Aguado, A. S. (2008). *Feature Extraction & Image Processing*. London: Academic Press.

Osowski, S., Siroić, R., Markiewicz, T., & Siwek, K. (2009). Application of Support Vector Machine and Genetic Algorithm for Improved Blood Cell Recognition. *IEEE Trans. Meas. and Instrum*, *58*, 2159–2168. doi:10.1109/TIM.2008.2006726

Schurmann, J. (1996). *Pattern classification, a unified view of statistical and neural approaches*. New Jersey: Wiley.

Semmlow, J. L. (2004). *Biosignal and Medical Image Processing*. New York: Marcel Dekker.

Spyridonos, P., Cavoura, D., Ravazoula, P., & Nikiforidis, G. (2002). Neural network based segmentation and classification system for automatic grading of histologic section of bladder carcinoma. *Analytical and Quantitative Cytology*, *24*, 317–324.

Stork, D., & Tov, E. Y. (2004). *Computer Manual in MATLAB to Accompany Pattern Classification*. New Jersey: Wiley.

Sugiyama, M. (2007). Dimensionality Reduction of Multimodal Labeled Data by Local Fisher Discriminant Analysis. *Journal of Machine Learning Research*, *8*, 1027–1061.

Tan, P. N., Steinbach, M., & Kumar, V. (2008). *Introduction to data mining*. New York: Pearson.

Young, I. T. (1996). Quantitative Microscopy. *IEEE Engineering in Medicine and Biology*, *15*, 59–66. doi:10.1109/51.482844

Zhang, Y. J. (2008). *Image Engineering - Processing, Analysis, and Understanding*. Hongkong, Cengage Learning.